# Determination of Xenon Valence and Conduction Bands by Spin-Polarized Photoemission

B. Kessler,[1] A. Eyers,[1,a] K. Horn,[2] N. Müller,[1] B. Schmiedeskamp,[1] G. Schönhense,[1] and U. Heinzmann[1]

[1]*Fakultät für Physik, Universität Bielefeld, D-4800 Bielefeld, West Germany*

[2]*Fritz-Haber-Institut der Max-Planck Gesellschaft, D-1000 Berlin 33, West Germany*

(Received 12 May 1987)

Using circularly polarized synchrotron radiation and spin-resolved photoemission, we have studied the valence and conduction bands of Xe(111) up to about 18 eV above the valence-band maximum. Direct information about the symmetry of bands and their hybridization is provided by photoelectron spin polarization. Our data also prove the existence of a gap in the unoccupied bands above the fundamental gap. A comparison of our data with calculated band structures shows the importance of an energy-dependent self-energy correction.

PACS numbers: 71.25.Tn, 79.60.Eq

The electronic band structure of a solid is central to an understanding of its physical properties. Great progress in the determination of valence-band structures has been achieved through the use of angle-resolved photoemission in combination with linearly polarized synchrotron radiation, with use of dipole selection rules. However, electronic bands of the heavier-element solids are less easily accessible with this technique since the bands are affected by spin-orbit interaction, and it has been shown[1] that when one uses linearly polarized light, the selection rules are relaxed to an extent which forbids a proper assignment of band symmetry species. This difficulty does not occur when circularly polarized light is used for photoexcitation and the electron spin polarization (ESP) is detected, as was demonstrated in studies of the valence-band structure of Pt[2] and Ir.[3]

Experimental band-structure determinations have so far concentrated on metals and elemental as well as compound semiconductors.[4] Here we present an experimental study of the band structure of the insulator xenon, and compare our results with existing band-structure calculations.[5-8]

The experiments were carried out on the 6.5-m normal-incidence monochromator[9] at the electron storage ring BESSY, Berlin, in an apparatus described previously.[2,10] All spectra were recorded for normal light incidence and normal electron emission; overall resolution (electrons plus photons) was better than 200 meV in the photon energy range which was used, at an angular resolution of $\pm 3°$. The Xe(111) crystals were epitaxially grown on Pt(111), Pd(111), and Ir(111) single-crystal substrates at temperatures of less than 50 K, and annealed at slightly higher temperatures. The growth of the crystalline Xe layers was controlled by observation of the structures of the photoemission peaks. Since we observe clear dispersion effects, and our spectra show good agreement with earlier studies using synchrotron radiation[6,11] and resonance lamps,[12] our results are characteristic of bulk Xe. The LEED pattern showed distinct spots of a (111) surface.

In Fig. 1 a typical spectrum of Xe(111) is shown at a photon energy of 12.5 eV. The top part shows the ESP. From the total intensity $I_0$ and the ESP $P$ the partial intensities $I_+$ and $I_-$ are obtained through

$$I_+ = \tfrac{1}{2} I_0(1+P), \quad I_- = \tfrac{1}{2} I_0(1-P). \tag{1}$$

For pure $\Lambda_6^1$ final states $I_+$ and $I_-$ are directly correlated with transitions starting from initial states with symmetries $\Lambda_6^3$ and $\Lambda_{4,5}^3$.[3] (Positive $P$ means that photon and electron spins are parallel.[13]) The total and partial in-

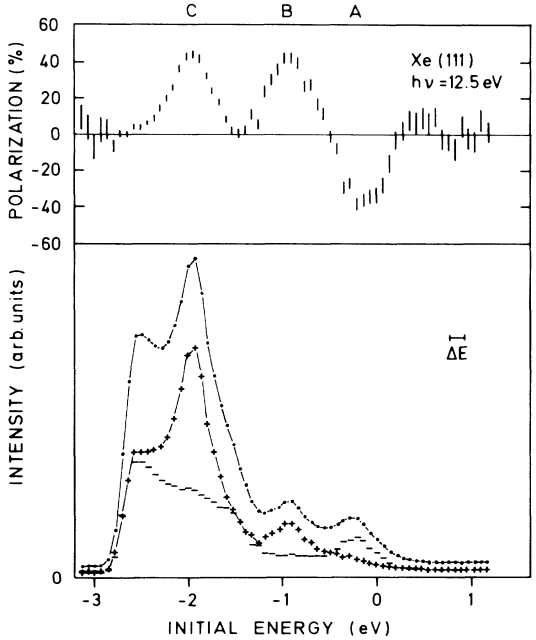


FIG. 1. Photoelectron polarization profile (upper part) and intensity spectrum (lower part, dots), recorded at a photon energy of 12.5 eV. Error bars for ESP show the total error including the uncertainty of light polarization and detector asymmetry function. + and − indicate partial intensities $I_+$ and $I_-$.

tensities are shown in the bottom of Fig. 1. Peaks labeled $A$, $B$, and $C$ can be clearly identified in the ESP and intensity curves. The initial energies of the peaks are given with respect to the valence-band maximum (VBM) of solid Xe. As a reference we used the vacuum level at 9.8 eV above VBM.[11]

Total-intensity spectra over a range of photon energies are shown in Fig. 2, normalized with respect to the photon flux. They and the ESP data are interpreted in terms of the band structure shown in Fig. 3. In solid Xe, the bottom of the first conduction band is located below the vacuum level.[11,14,15] Thus the direct photoemission sets in when the photon energy matches the distance of the topmost occupied band to the crossing of the first conduction band with the vacuum level. Since peaks at the low-energy cutoff are difficult to determine, we take the first data points from the clearly dispersing feature about 0.5 eV above the cutoff. The remarkable intensity decrease of peak $A$ in going from $h\nu = 11.4$ eV to $h\nu = 11.8$ eV (cf. Fig. 2) is explained by a gap which opens up above the first conduction band. With further increase of photon energy, the peaks at lower initial energy experience the same drastic intensity decrease.

The spectra of Fig. 2 also reveal the presence of features which appear at a constant kinetic energy caused by excited electrons which have suffered an energy loss and are subsequently emitted from points of high density of states in the *unoccupied* part of the band structure (e.g., $L_6^+$ and $X_6^+$). Other peaks in the spectra appear at a constant initial energy (e.g., at $-2.5$ eV).

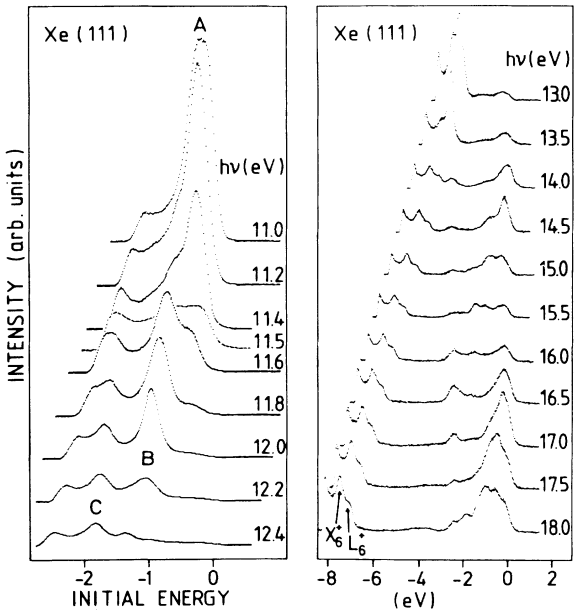


FIG. 2. Photoelectron intensity spectra at photon energies between 11.0 and 18.0 eV. The spectra are normalized with respect to the photon flux. The spectra above $h\nu = 13.0$ eV are enlarged by a factor 5.

These are related to emission from critical points in the *occupied* band structure through nondirect transitions, and are thus included in our determination of the $\Gamma$ and $L$ points and of the width of the occupied bands.

The occupied part of the band structure of Xe has a simple shape because only the $5p$ states contribute to it.[5,6,8] At $\Gamma$, spin-orbit interaction leads to a splitting of the $\Gamma_{15}$ level into $\Gamma_8^-$ and $\Gamma_6^-$ [see Fig. 3(b)]. From the maximum energy shift of the peaks in the spectra, we obtain a value for the total bandwidth of 1.0 eV for the

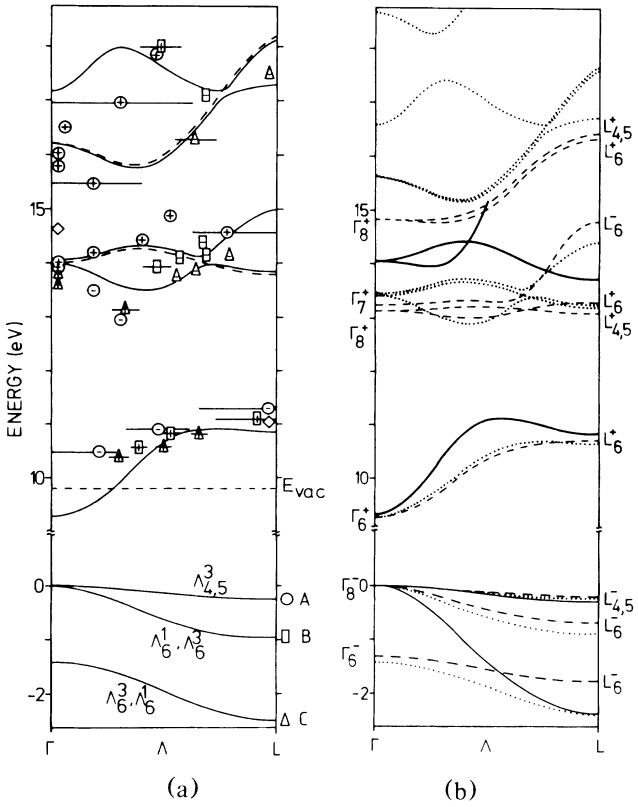


FIG. 3. Comparison of experimental results and band structure calculations: (a) Data points (circles, squares, and triangles) represent direct transitions from bands $A$, $B$, and $C$; signs indicate the sign of the observed ESP. Lozenges indicate density of states emission (see text). Error bars show typical uncertainties in $k$ resulting from small dispersions. The unoccupied bands are the relativistic LAPW bands of Noffke and Hermann (Ref. 7) adjusted to the self-energy corrected local-density-approximation calculation of Timmer and Borstel (Ref. 8) (see text). $\Lambda_{4,5}^3$ bands are shown as dashed lines since electron emission via these states into the vacuum is not possible (Ref. 17). Occupied bands, see text. (b) Comparison of three band-structure calculations of Xe along $\Gamma$-$L$. Dashed lines show Korringa-Kohn-Rostoker bands of Rössler (Ref. 5), dotted lines the linear rigorous cellular LAPW bands of Noffke and Hermann (Refs. 6 and 7) with conduction bands shifted by 3.15 eV towards higher energies in order to adjust to the optical gap. Full lines give the bands by Timmer and Borstel (Ref. 8). Symmetry labels were taken from Rössler (Ref. 5).

lowest band $C$, of 0.9 eV for the second band $B$, and of 0.25 eV for the top band $A$. These bandwidths are larger than the dispersion calculated by Rössler[5] using the Korringa-Kohn-Rostoker method, but agree fairly well with the linear rigorous cellular calculations by Horn *et al.*[6] Having determined not only the bandwidth but also the band positions at the Brillouin-zone boundaries experimentally, we base only the shape of the bands along $\Lambda$ on the calculated bands[6] [see Fig. 3(a)].

In most cases electronic band determinations through photoemission have been based on free-electron final states, and have concentrated on the occupied band structure. Bands directly above the fundamental gap in a large-gap material are by no means free-electron-like, however. Here, we use our semiempirical valence bands as a basis to obtain data points and symmetries of the unoccupied bands through the use of dipole selection rules for circularly polarized light.[16]

The result is displayed in Fig. 3(a). We obtain a first group of data points just above the vacuum level, a second group between 13 and 15 eV, and, as a third group, a few data points above 15 eV. This classification corresponds to the intensity variations of the peaks in Fig. 2. The first group of data points yields the course of the first conduction band above the vacuum level. Its minimum (below the vacuum level at $\Gamma$) is known accurately from photoabsorption data.[15] Transitions from band $A$ yield negative ESP, while the transitions from bands $B$ and $C$ both yield positive ESP.

From the selection rules[16] and the observed ESP we derive the result that the first conduction band is of $\Lambda_6^1$ symmetry, that valence band $A$ is of $\Lambda_{4,5}^3$ symmetry, and that bands $B$ and $C$ both must contain contributions of $\Lambda_6^3$ character. The latter is only possible if bands $B$ and $C$ are $\Lambda_6^1$-$\Lambda_6^3$ hybrids, originating from an avoided crossing of a $\Lambda_6^1$ band with a $\Lambda_6^3$ band. If band $B$ were of pure $\Lambda_6^1$ symmetry, it would not be observable in our experimental geometry.[17]

From the second and third group of data points we cannot deduce the course of the bands. One can, however, obtain the energy and, via the ESP, the symmetry character of the unoccupied bands. The lowest four points in the second group of bands are compatible with a $\Lambda_6^1$ band; all other points demand $\Lambda_6^1$-$\Lambda_6^3$ hybrids. A comparison of our experimental data points in Fig. 3(a) with three band-structure calculations [see Fig. 3(b)] is hampered by the fact that while the occupied bands of the relativistic calculations agree rather well with experiment, the fundamental gap is usually not well represented by theory[6,7] or is adjusted to the experimental value.[5] The self-energy–corrected local-density-functional calculation[8] successfully accounts for the optical gap to within 0.04 eV and is thus more reliable as far as the band energies are concerned. It does, however, not include spin-orbit splitting, which is a serious shortcoming for the occupied bands, since the size of the spin-orbit splitting of more than 1 eV in the occupied bands is comparable to the bandwidth. For the unoccupied bands, the splitting is almost an order of magnitude smaller,[5,7] and does not affect the energies significantly. An interesting point is the fact that if self-energy corrections are not taken into account, the nonrelativistic calculation of Timmer and Borstel[8] yields the same energetic positions of the unoccupied bands at the $\Gamma$ and $L$ points as the linearized augmented plane wave (LAPW) calculation by Noffke and Hermann (NH).[7] Since NH provide a fully relativistic calculation with bands up to 25 eV, we regard it as being more suitable for a comparison with our data. In order to conform with experiment, the fundamental gap in the calculation by NH had to be increased by about 50%. A comparison between NH's calculated bands [dotted in Fig. 3(b)] with our data points shows that an adjustment of only the fundamental gap fails to represent both the width of the first conduction band and the energy of the second group of bands. Agreement is improved if we apply the energy-dependent self-energy correction of Timmer and Borstel at $\Gamma_6^+$, $L_6^+$, and $\Gamma_8^+/\Gamma_7^+$ to the LAPW calculation.[7] Above 15 eV the NH bands are rigidly shifted in line with the second group of bands. As a result of this procedure, we obtain the lines drawn through the data points in Fig. 3(a). The calculated $\Lambda_6^1$-$\Lambda_6^3$ hybrids in the second and third groups are also consistent with the measured ESP.[18]

An observation which should also be noted is that weak emission from all three valence bands occurs in the gap region above the first conduction band (see Fig. 2). We ascribe these features to effects arising from deviations of our target from an ideal 3D single-crystalline solid, or to surface emission.

Recent inverse photoemission experiments from crystalline xenon[19,20] show emission which is interpreted as arising from points of high density of states in the conduction-band structure. Their energies agree well with the critical-point energies shown in Fig. 3(a).

In summary, we have shown that the first unoccupied band is $\Lambda_6^1$ character, with a width of $1.7 \pm 0.2$ eV. Above this first conduction band we find a gap of approximately 2-eV width, followed by a broad region with strongly hybridized $\Lambda_6^1$-$\Lambda_6^3$ bands. Agreement with calculations for the unoccupied bands is improved when an energy-dependent self-energy correction is taken into account, pointing to the importance of such corrections for a description of excited states of the solid. We also show that the first and second valence bands [$C$ and $B$ in Fig. 3(a)] result from an avoided crossing of $\Lambda_6^1$ and $\Lambda_6^3$ bands.

We would like to thank M. Timmer and G. Borstel, as well as J. Noffke and K. Hermann, for making their calculations available to us prior to publication. We also express our thanks to A. M. Bradshaw and K. Kambe for stimulating discussions, to U. Friess for his expert technical assistance, to the staff of BESSY for their help,

and to T. N. Rhodin and B. Addis for the Ir(111) crystal. This work was supported by the Bundesministerium für Forschung und Technologie through Grant No. 05 331 AX.

---

[a]Present Address: Philips GmbH, D-2000 Hamburg, West Germany.

[1]G. Borstel, M. Neumann, and M. Wöhlecke, Phys. Rev. B **23**, 3121 (1981); G. Borstel, Appl. Phys. A **38**, 193 (1985).

[2]A. Eyers, F. Schäfers, G. Schönhense, U. Heinzmann, H. P. Oepen, K. Hünlich, J. Kirschner, and G. Borstel, Phys. Rev. Lett. **52**, 1559 (1984).

[3]N. Müller, B. Kessler, B. Schmiedeskamp, G. Schönhense, and U. Heinzmann, Solid State Commun. **61**, 187 (1987).

[4]F. J. Himpsel, Adv. Phys. **32**, 1 (1983).

[5]U. Rössler, Phys. Status Solidi (b) **42**, 345 (1970).

[6]K. Horn, A. M. Bradshaw, J. Noffke, and K. Hermann, in *Proceedings of the Sixth Vacuum Ultraviolet Radiation Physics Conference, Charlottesville, 1980, Extended Abstracts* (U.S. Naval Research Laboratory, Washington, D.C., 1980), Abstract I32.

[7]J. Noffke and K. Hermann, private communication (LAPW; unoccupied bands).

[8]M. Timmer and G. Borstel, to be published. The quasiparticle band structure of Xe has been calculated in the framework of the quasiparticle local-density approximation as proposed by W. E. Pickett and C. S. Wang, Phys. Rev. B **30**, 4719 (1984).

[9]F. Schäfers, W. Peatman, A. Eyers, Ch. Heckenkamp, G. Schönhense, and U. Heinzmann, Rev. Sci. Instrum. **57**, 1032 (1986).

[10]G. Schönhense, A. Eyers, U. Friess, F. Schäfers, and U. Heinzmann, Phys. Rev. Lett. **54**, 547 (1985).

[11]N. Schwentner, F. J. Himpsel, V. Saile, M. Skibowski, W. Steinmann, and E. E. Koch, Phys. Rev. Lett. **34**, 528 (1975).

[12]K. Horn, A. M. Bradshaw, Solid State Commun. **30**, 545 (1979).

[13]This convention is the convention used in photoemission from free and adsorbed atoms. It is in the opposite sense to the convention used in Refs. 2 and 3.

[14]E. T. Steinberger, E. H. Munro, E. Pantos, and U. Asaf, *Vacuum UV Radiation Physics* (Pergamon-Vieweg, Braunschweig, 1974).

[15]U. Rössler, in *Rare Gas Solids,* edited by M. K. Klein and J. A. Venables (Academic, London, 1976), Vol. 1; B. Sonntag, in *Rare Gas Solids,* edited by M. K. Klein and J. A. Venables (Academic, London, 1977), Vol. 2.

[16]M. Wöhlecke and G. Borstel, in *Optical Orientation,* edited by F. Meier and B. P. Zakharchenya (Elsevier, Amsterdam, 1984).

[17]J. Hermanson, Solid State Commun. **22**, 9 (1977).

[18]For the interpretation of the data it should be noted that the dots in Tables 3–10 of Ref. 16 indicate either a vanishing matrix element or a vanishing ESP. For the transition $\Lambda_6^3 \rightarrow \Lambda_6^3$ (in Table 4) the ESP is zero while the matrix element is nonzero.

[19]E. Bertel, W. Jacob, and V. Dose, to be published.

[20]K. H. Frank, K. Horn, J. Wilder, and E. E. Koch, to be published.